Analytic free-form lens design in 3D: coupling three ray sets using two lens surfaces

Fabian Duerr,[1,*] **Pablo Benítez,**[2,3] **Juan C. Miñano,**[2,3] **Youri Meuret,**[1] **and Hugo Thienpont**[1]

[1]*Brussels Photonics Team, Vrije Universiteit Brussel, Pleinlaan 2, B-1050 Brussels, Belgium*
[2]*CeDInt, Universidad Politécnica de Madrid (UPM), Campus de Montegancedo, 28223 Pozuelo, Madrid, Spain*
[3]*LPI, 2400 Lincoln Ave., Altadena, CA 91001 USA*
[*]*fduerr@b-phot.org*

Abstract: The two-dimensional analytic optics design method presented in a previous paper [Opt. Express **20**, 5576–5585 (2012)] is extended in this work to the three-dimensional case, enabling the coupling of three ray sets with two free-form lens surfaces. Fermat's principle is used to deduce additional sets of functional differential equations which make it possible to calculate the lens surfaces. Ray tracing simulations demonstrate the excellent imaging performance of the resulting free-form lenses described by more than 100 coefficients.

OCIS codes: (080.2720) Mathematical methods; (080.2740) Geometric optical design.

References and links

1. F. Duerr, P. Benítez, J.C. Miñano, Y. Meuret, and H. Thienpont, "Analytic design method for optimal imaging: coupling three ray sets using two free-form lens profiles," Opt. Express **20**, 5576–5585 (2012).
2. J.C. Miñano, P. Benítez, W. Lin, J. Infante, F. Muñoz, and A. Santamaría, "An application of the SMS method for imaging designs," Opt. Express **17**, 24036–24044 (2009).
3. P. Benítez, J.C. Miñano, J. Blen, R. Mohedano, J. Chaves, O. Dross, M. Hernández, and W. Falicoff, "Simultaneous multiple surface optical design method in three dimensions," Opt. Eng. **43**, 1489 (2004).
4. D. Grabovičkić, P. Benítez, and J.C. Miñano, "Free-form V-groove reflector design with the SMS method in three dimensions," Opt. Express **19**, A747–A756 (2011).

1. Introduction

In recently published work, a new analytic two-dimensional optics design method was proposed that enables the coupling of three ray sets with two aspheric lens profiles, especially important for imaging systems designed for a wide field of view and with clearly separated optical surfaces. The full three-dimensional solution presented in this paper builds directly on the already derived two-dimensional solution [1].

One explicit two-dimensional solution of such lens profiles is shown in Fig. 1(a), which perfectly focus three sets of parallel rays with incident angles -12°, 0° and 12° onto three points. Based on the 2D lens profile solutions, there are different possibilities to construct three-dimensional lens surfaces. The most obvious choice is a rotational symmetric lens, as it is shown in Fig. 1(b). The two-dimensional lens profiles (indicated by solid lines) are rotated about the optical axis. Rotational symmetry greatly simplifies the design process and analysis

#164359 - $15.00 USD Received 7 Mar 2012; revised 13 Apr 2012; accepted 18 Apr 2012; published 25 Apr 2012

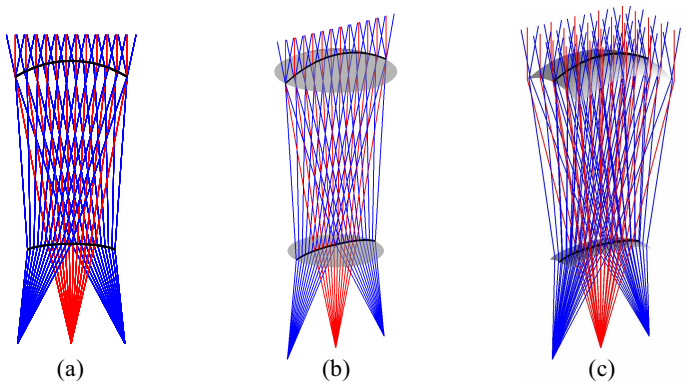

Fig. 1. (a) Exemplary lens calculated with the previously published two-dimensional design method that couple three rays sets; (b) rotational symmetric lens constructed from such two-dimensional design; (c) free-form lens design designed in this paper to couple three ray sets in three dimensions

of optical systems. The rotational symmetry of the optical system usually makes it the best solution for design problems where the object and image are rotational symmetric with respect to the optical axis, despite the fact that only the normal incidence rays and the tangential ray fans at the design angles $\pm\theta$ will have perfect focusing [2]. In practice, this design approach is also sufficient to meet the specifications for systems with rectangular field of view and rectangular image receivers characterized by moderate aspect ratios.

In the case of high aspect ratio, rotational symmetric solutions are not optimal, particularly in the limit of an infinite aspect ratio, in which the field of view consists of coplanar directional vectors and the correspondent image receiver reduces to a line. In this particular case, our solution here, illustrated in Fig. 1(c), is more suitable. It shares similarities with the Simultaneous Multiple Surface method in three dimensions (SMS3D) which provides an optical system with two free-form surfaces that deflects two input ray sets with opposite signs into two corresponding output ray sets and vice versa [3]. For optical systems designed for a wide field of view and with clearly separated optical surfaces, the three-dimensional free-form lens design method discussed in this paper will allow the coupling of an additional on-axis (parallel to the optical axis) ray set to the correspondent image point. Its cross section in x-z-plane (the solid lines in Fig. 1(c)) is given by the two-dimensional design method and provides a partial solution (depending on x-coordinate only) to the full three-dimensional problem.

To calculate all further coefficients having a y-coordinate dependency, Fermat's principle is used in Sec. 2 to deduce a system of functional differential equations in two variables by using the previously established concept of convergence points [1]. A first three-dimensional implementation of convergence points has been used to design free-form V-groove reflectors [4]. The transformation into two linear systems of equations allows the successive calculation of the analytic Taylor series coefficients in two variables up to an arbitrary order. Ray tracing analysis in Sec. 3 is used to demonstrate the versatility of this analytic design approach by explicitly evaluating high-order Taylor polynomials in two variables, described by 65 coefficients for each surface.

2. Analytic free-form solution starting from convergence points

In the previously published paper [1] on the two-dimensional problem, the concept of convergence points has been used to derive an algebraic solution scheme. As one main result it has

#164359 - $15.00 USD Received 7 Mar 2012; revised 13 Apr 2012; accepted 18 Apr 2012; published 25 Apr 2012

been shown that this 2D design can be fully described by two variables only, the slopes m_0 and m_1 at the convergence points. This basic construction for one on-axis and one off-axis ray set will serve as the starting point for the three-dimensional problem as well. Figure 2(a) shows the convergence points construction in analogy to the two-dimensional problem.

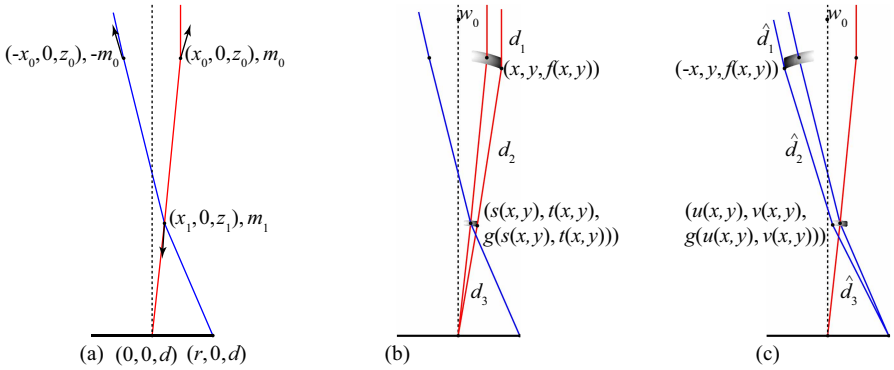

Fig. 2. Introduction of all necessary initial values and functions to derive the conditional equations from Fermats principle in three dimensions

The convergence point on the upper surface has the point coordinates $(\pm x_0, y_0, z_0)$ with $y_0 = 0$ due to the overall lens' mirror symmetry with respect to the *x*-*z*- and *y*-*z*- plane. Therefore, the normal vector at the first convergence point is completely described by the single variable m_0. The intersection of the refracted on-axis ray through $(x_0, 0, z_0)$ and the refracted off-axis ray through the mirrored convergence point $(-x_0, 0, z_0)$ determines the coordinates $(x_1, 0, z_1)$ of the second convergence point. The normal vector at the second convergence point is also described by a the single variable m_1. Further refractions at the second convergence point result in the focus positions $(0,0,d)$ and $(r,0,d)$. The initial ray construction lies within the sectional plane $y = 0$ of the lens and corresponds exactly to the two-dimensional construction.

Next, all necessary functions describing the optical system have to be introduced. Therefore, two explicit surface functions $z = f(x,y)$ and $z = g(x,y)$ are defined to describe the lens surfaces. To completely describe the optical paths of rays passing through the lens surfaces, it is necessary to introduce additional mapping functions. In two dimensions, two mapping functions $s(x)$ and $u(x)$ were sufficient to define the mapping in *x*-coordinate. For the full three-dimensional problem it is necessary to define two additional mapping functions in *y*-coordinate, for on- and off-axis rays, respectively. This results in the overall mapping functions $s(x,y)$ and $t(x,y)$ for on-, and $u(x,y)$ and $v(x,y)$ for off-axis rays, and for *x*-direction and *y*-direction, respectively.

Figure 2(b) shows an on-axis ray passing through an arbitrary point $\vec{p}_1 = (x, y, f(x,y))$ on the upper lens surface which is then refracted in $\vec{p}_2 = (s(x,y), t(x,y), g(s(x,y), t(x,y)))$ towards the focal point $\vec{p}_3 = (0,0,d)$. Figure 2(c) shows an off-axis ray passing through an arbitrary point $\hat{\vec{p}}_1 = (-x, y, f(x,y))$ on the upper lens surface which is then refracted in $\hat{\vec{p}}_2 = (u(x,y), v(x,y), g(u(x,y), v(x,y)))$ towards the focal point $\hat{\vec{p}}_3 = (r,0,d)$. Similarly to the 2D result, all optical path lengths can be expressed in sections using vector geometry as

$$d_1 = \vec{v}_0 \cdot (\vec{p}_1 - \vec{w}_0), \qquad d_2 = n_2 |\vec{p}_2 - \vec{p}_1|, \qquad d_3 = |\vec{p}_3 - \vec{p}_2| \tag{1}$$

for on axis rays, and as

$$\hat{d}_1 = \vec{v}_1 \cdot (\hat{\vec{p}} - \vec{w}_0), \qquad \hat{d}_2 = n_2 |\hat{\vec{p}}_2 - \hat{\vec{p}}_1|, \qquad \hat{d}_3 = |\hat{\vec{p}}_3 - \hat{\vec{p}}_2| \tag{2}$$

#164359 - $15.00 USD Received 7 Mar 2012; revised 13 Apr 2012; accepted 18 Apr 2012; published 25 Apr 2012

for off-axis rays. The vectors $\vec{v}_0$ and $\vec{v}_1$ denote the directional vectors for on- and off-axis ray sets, respectively. The position vector $\vec{w}_0$ denotes an arbitrary but fixed point on both plane wave-fronts and n_2 denotes the refractive index of the lens.

Fermat's principle is now applied to calculate the remaining terms having a y-coordinate dependency. Therefore, additional conditional equations are required and defined as

$$D_1 = \frac{\partial}{\partial y}(d_1 + d_2) = 0, \qquad D_2 = \frac{\partial}{\partial s}(d_2 + d_3) = 0, \qquad D_3 = \frac{\partial}{\partial t}(d_2 + d_3) = 0 \tag{3}$$

for on-axis, and as

$$D_4 = \frac{\partial}{\partial y}(\hat{d}_1 + \hat{d}_2) = 0, \qquad D_5 = \frac{\partial}{\partial u}(\hat{d}_2 + \hat{d}_3) = 0, \qquad D_6 = \frac{\partial}{\partial v}(\hat{d}_2 + \hat{d}_3) = 0 \tag{4}$$

for off-axis rays, using identical arguments as in [1]. The lens design as introduced in Fig. 2 is then fully described by four functional differential equations derived for the two-dimensional problem, plus six Eqs. (3) and (4) for six unknown surface functions $f(x,y), g(x,y), s(x,y), t(x,y), u(x,y)$ and $v(x,y)$. To our knowledge, the existence and uniqueness of solutions to similar systems of functional differential equations in two variables have not been discussed in detail nor proven up to now.

Supposing that there exists an analytic and smooth solution (f,g,s,t,u,v) to the functional differential Eqs. (3) and (4), Taylors theorem implies that the functions must be infinitely differentiable and have a power-series representation in two variables. Thus the six functions can be given by power-series

$$f(x,y) = \sum_{i=0}^{\infty}\sum_{j=0}^{\infty} f_{i,j}(x-x_0)^i y^{2j}, \qquad g(x,y) = \sum_{i=0}^{\infty}\sum_{j=0}^{\infty} g_{i,j}(x-x_1)^i y^{2j} \tag{5}$$

$$s(x,y) = \sum_{i=0}^{\infty}\sum_{j=0}^{\infty} s_{i,j}(x-x_0)^i y^{2j}, \qquad u(x,y) = \sum_{i=0}^{\infty}\sum_{j=0}^{\infty} u_{i,j}(x-x_0)^i y^{2j} \tag{6}$$

$$t(x,y) = \sum_{i=0}^{\infty}\sum_{j=1}^{\infty} t_{i,j}(x-x_0)^i y^{(2j-1)}, \qquad v(x,y) = \sum_{i=0}^{\infty}\sum_{j=1}^{\infty} v_{i,j}(x-x_0)^i y^{(2j-1)} \tag{7}$$

centered at convergence points $(x_0,0,z_0)$ and $(x_1,0,z_1)$, respectively. The exponents for y-coordinate take already into account that all functions are either even (provided by $2j$) or odd (provided by $2j-1$) in y-direction.This symmetry follows immediately from the later introduced Eqs. (9) and (10). The linear systems of equations for the correspondent Taylor series coefficients have null vectors as only possible solutions and are therefore discarded already in the Taylor series. The coefficients $f_{i,0}$, $g_{i,0}$, $s_{i,0}$ and $u_{i,0}$ can be identified as the already calculated Taylor series coefficients with the two-dimensional optics design method. The in Fig. 2(a) introduced and in Eqs. (5)-(7) assigned initial conditions

$$\begin{aligned}
&f(x_0,0) = z_0, \qquad \partial_x f(x,y)\big|_{(x_0,0)} = m_0, \qquad \partial_y f(x,y)\big|_{(x_0,0)} = 0 \\
&g(x_1,0) = z_1, \qquad \partial_x g(x,y)\big|_{(x_1,0)} = m_1, \qquad \partial_y g(x,y)\big|_{(x_1,0)} = 0 \\
&s(x_0,0) = x_1, \qquad u(x_0,0) = x_1, \qquad t(x_0,0) = 0, \qquad v(x_0,0) = 0
\end{aligned} \tag{8}$$

then satisfy the conditional equations $D_i = 0$ for $i = 1..6$ and provide general solutions for the initial Taylor series coefficients depending upon variables m_0 and m_1. The overall solution for arbitrary order can be calculated by solving four equations

$$\lim_{x\to x_0}\lim_{y\to 0}\frac{\partial^n}{\partial x^n}\frac{\partial^m}{\partial y^m} D_i = 0 \quad (i = 1,3,4,6), \quad \{n = 0, m \in \mathbb{N} | \text{odd number } m\} \tag{9}$$

#164359 - $15.00 USD Received 7 Mar 2012; revised 13 Apr 2012; accepted 18 Apr 2012; published 25 Apr 2012

for y-coordinate dependency, and six equations

$$\begin{aligned}
&\lim_{x\to x_0}\lim_{y\to 0}\frac{\partial^n}{\partial x^n}\frac{\partial^m}{\partial y^m}D_i = 0 \quad (i=1,3,4,6), \quad \{n\in\mathbb{N}_1, m\in\mathbb{N}|\text{odd number } m\}\\
&\lim_{x\to x_0}\lim_{y\to 0}\frac{\partial^{n-1}}{\partial x^{n-1}}\frac{\partial^{m+1}}{\partial y^{m+1}}D_i = 0 \quad (i=2,5), \quad \{n\in\mathbb{N}_1, m\in\mathbb{N}|\text{odd number } m\}
\end{aligned} \tag{10}$$

for mixed x-y-coordinate dependency. Provided that the solution for the two-dimensional problem is known, there are again two cases needed to be solved:

1. For $m=1$, the set of Eq. (9) results in four nonlinear algebraic equations for Taylor series coefficients $f_{0,2}$, $g_{0,2}$, $t_{0,1}$ and $v_{0,1}$. These equations have two general solutions, where one solution can be discarded as non-physical. The remaining unique solution can be expressed as functions of the initial, already known Taylor coefficients.

2. For $m\geq 1$ and $n\geq 1$, it is useful to introduce an ordinal number $o=m+n$. The sets of Eqs. (9) and (10) result in two systems of linear equations for particular Taylor series coefficients which can be expressed as compact matrix equations

$$M_y\begin{pmatrix} f_{0,m+1}\\ g_{0,m+1}\\ t_{0,m}\\ v_{0,m}\end{pmatrix} = \vec{b}^{(0,m)} \tag{11}$$

for y-coordinate dependency, and

$$M_{xy}\begin{pmatrix} f_{n,m+1}\\ g_{n,m+1}\\ s_{n-1,m+1}\\ t_{n,m}\\ u_{n-1,m+1}\\ v_{n,m}\end{pmatrix} = \vec{b}^{(n,m)} \tag{12}$$

for x-y-coordinate dependency and for arbitrary $o\geq 2$. The matrix elements of M_y and M_{xy} consist of mathematical expressions which depend on Taylor series coefficients calculated for the initial conditions. The needed vector elements of $\vec{b}^{(n,m)}$ for $o=n+m$ are mathematical expressions only dependent on previously calculated Taylor series coefficients for $o=2,3,..,(n+m-1)$ and can be calculated for each ordinal number $o=2,3,..$ in ascending order and for all possible combinations of n and m from Eqs. (9) and (10). For known matrices M_y and M_{xy} and vectors $\vec{b}^{(n,m)}$, the Taylor series coefficients can be calculated by solving the linear systems of Eqs. (11) and (12).

These algebraic steps of calculation provide a scheme to calculate Taylor polynomial coefficients from Eqs. (5)-(7) with a y-coordinate dependency ($j\geq 1$) up to an arbitrary but finite order. Taylors remainder theorem in two variables provides quantitative estimates on convergence and the approximation error of the functions by its Taylor polynomials. The radii of convergence for the expansions $f(x,y)$ and $g(x,y)$ are very important, as they indicate the maximum aperture that can be achieved for a given set of initial values. In the examples considered, the radius of convergence is larger than the range of $0<x<x_{max}$ and $0<y<y_{max}$ of the lenses. The presented calculation is fully implemented in Wolfram *Mathematica*.

#164359 - $15.00 USD Received 7 Mar 2012; revised 13 Apr 2012; accepted 18 Apr 2012; published 25 Apr 2012

3. Ray tracing results for calculated high-order Taylor polynomials of two variables

All calculated mathematical expressions (including the previously calculated coefficients for x-coordinate dependency in [1]), sorted in the right order, are exported as `C++` compatible code and embedded in a MATLAB-compatible `mex` file library. Once compiled, this library returns the calculated Taylor polynomial coefficients for the lens surfaces $f(x,y)$ and $g(x,y)$ and the mapping functions $s(x,y)$, $t(x,y)$, $u(x,y)$ and $v(x,y)$ for input parameters (θ, m_0, m_1, n_2). For x-coordinate dependency, the coefficients were previously calculated up to 15^{th} order.

The remaining terms with y-coordinate dependency are calculated up to $o = 13$, resulting in a total number of 65 Taylor coefficients for $f(x,y)$ and $g(x,y)$, respectively. This derived general three-dimensional calculation provides solutions for any given (physically meaningful) initial parameter set (θ, m_0, m_1, n_2).

The fact that the cross-sectional 2D solution is part of the 3D solution is used to calculate m_0 and m_1 for fixed design angle $\theta = 12^\circ$ and refractive index $n_2 = 1.5$ with the two-dimensional optics design method, ensuring that the boundary condition at the optical axis is fulfilled. For each pair of variates, the full three-dimensional solution is then determined. The present quadrant symmetry of the calculated lens surfaces is not further imposed; it rather follows naturally from the calculated solutions. We cannot provide a mathematical proof but only state that the so far calculated free-form surfaces are always quadrant symmetric, as long as the boundary condition of the 2D solution $f'(0) = g'(0) = 0$ is fulfilled.

A ray tracing animation video (Media 1) illustrates the correlation between m_0 and m_1 in three dimensions. The slope value m_1 ranges from -0.065 to 0.045. For higher values, all Taylor polynomial coefficients with a y-coordinate component become imaginary and the three-dimensional lens construction fails. Figure 3 shows two single-frame excerpts from this ray tracing animation video for $m_1 = -0.065$ which is equivalent to a meniscus lens (a), and $m_1 = 0.045$ which is equivalent to a biconvex lens (b). The two arrows indicate the directions of the normal vectors at the convergence points.

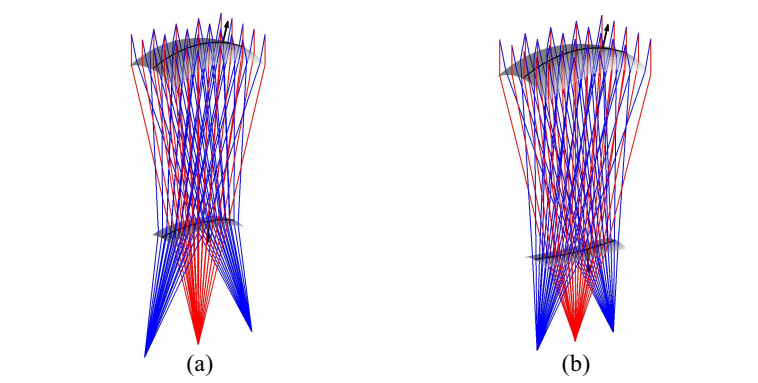

Fig. 3. Exemplary single-frame excerpts from a ray tracing animation of calculated solutions ranging from meniscus lenses (a) to biconvex lenses (b) (Media 1)

The ray tracing simulations for this animation video (240 frames) are done using the MATLAB-based ray tracer OPS (by courtesy of Prof. Dr. Udo Rohlfing, Hochschule Darmstadt, Germany). As it currently does not provide ray tracing for explicit surfaces, $f(x,y)$ and $g(x,y)$ are approximated by tensor product B-spline surfaces of 3^{rd} order defined over an x-y-grid. To avoid occurring approximation errors in the future, an extension of OPS or the use of a commercial ray tracer will be considered. To evaluate the imaging performance in three dimensions with OPS, the RMS spot radius is analyzed as a function of the incident direction

#164359 - $15.00 USD Received 7 Mar 2012; revised 13 Apr 2012; accepted 18 Apr 2012; published 25 Apr 2012

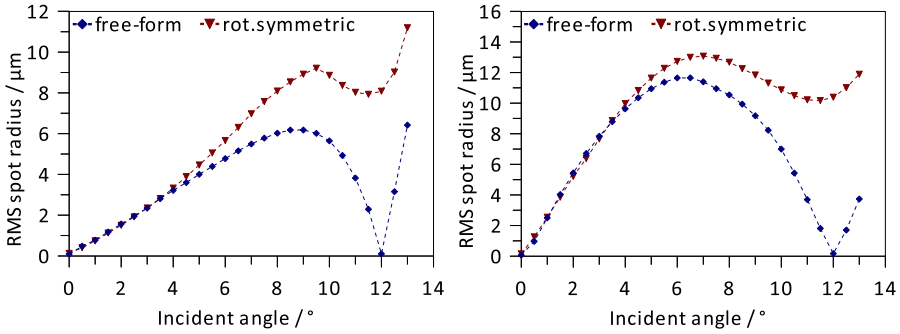

Fig. 4. RMS spot radius plotted against the incident angle for $m_1 = -0.065$ (a) and for $m_1 = 0.045$ (b) and for corresponding free-form and rotational symmetric lenses

in x-z-plane and for monochromatic light (corresponding to $n_2 = 1.5$) with the object points at infinity (i.e., parallel rays). The ray tracing results of Fig. 4(a) and 4(b) show the RMS spot radius plotted against the incident angle in 0.5° steps for two different pairs of variates m_0 and m_1 and the corresponding rotational symmetric and free-form lenses.

Figure 4(a) shows results for $m_1 = -0.065$ for the calculated free-form lens as shown in Fig. 3(a), and for the rotational symmetric equivalent based on the two-dimensional design method as shown in Fig. 1(b). Figure 4(b) shows the same evaluation for $m_1 = 0.045$. Both rotational symmetric lenses have an entrance diameter of 3.8mm; the upper surfaces of the free-form lenses have dimensions of 3.8mm$\times$2.92mm, ensuring approximately identical entrance aperture surface areas. The f-numbers of the rotational symmetric lenses are f/2.7 for the meniscus, and f/1.9 for the biconvex lens. The free-form lenses have identical f-numbers in x-direction for the meniscus and the biconvex lens, respectively. In y-direction, the f-numbers are f/3.4 for the meniscus, and f/3.2 for the biconvex free-form lens. The four mapping functions $s(x,y)$, $t(x,y)$, $u(x,y)$ and $v(x,y)$ enable a precise tailoring of the lower lens surfaces, ensuring that all rays going through the first lens surface also reach the receiver plane.

As expected, the RMS spot radii at the design angle 0° in case of the rotational symmetric lenses and at the design angles 0° and $\pm 12^\circ$ in case of the free-form lenses are almost zero (of the order of 0.05 microns). The analysis for intermediate incident directions demonstrate a considerably better performance for the meniscus over the biconvex lenses. In direct comparison, the free-form lenses provide a better overall imaging performance when compared with its rotational symmetric counterparts. It should be noted that for incident angles beyond 12°, not all rays going through the first lens surface reach the receiver plane anymore.

These graphs provide a first quantitative analysis of the intermediate image performance. However, the here considered thick lenses are primarily used as a proof of principle. After the successful demonstration of this new optics design method allowing to simultaneously calculate two free-form surfaces, future work will focus on real world applications for which this method can tap its full potential. Therefore, it might be necessary to consider more than two surfaces, different symmetry considerations and generalized wave-fronts for objects at a finite distance.

4. Conclusion

Within the scope of this work, the previously presented two-dimensional design method enabling the coupling of three ray sets with two refractive surfaces has been successfully extended

#164359 - $15.00 USD Received 7 Mar 2012; revised 13 Apr 2012; accepted 18 Apr 2012; published 25 Apr 2012

to three dimensions. The established convergence point formalism and Fermat's principle provided the basis for an analytical description enabling the simultaneous calculation of two free-form lens surfaces. The derived set of functional differential equations led to algebraic systems of equations which can be solved up to an arbitrary order. Exemplary ray tracing results for calculated lens surfaces given as high order Taylor polynomials of two variables demonstrated the capabilities and versatility of this new analytical optics design method. Future work will target applications where this new three-dimensional optics design method is particularly promising and will help to further increase the overall optical system's performance.

Acknowledgments

Work reported in this paper is supported in part by the Research Foundation - Flanders (FWO-Vlaanderen) that provides a PhD grant (grant number FWOTM510) and provided a grant for a research period at CeDInt, Universidad Politécnica de Madrid (grant number V424711N) for Fabian Duerr, and in part by the IAP BELSPO VI-10, the Industrial Research Funding (IOF), Methusalem, VUB-GOA, and the OZR of the Vrije Universiteit Brussel. Work is also supported by projects TEC2011-24019 and SEM: TSI-020302-2010-65, funded by the Spanish Ministries MEC and MITYC, respectively.

#164359 - $15.00 USD Received 7 Mar 2012; revised 13 Apr 2012; accepted 18 Apr 2012; published 25 Apr 2012